Surf. Sci. Spectra 30, 014004 (2023); https://doi.org/10.1116/6.0002280

XPS analysis of graphitic carbon nitride functionalized with CoO and $CoFe_2O_4$

Mattia Benedet,[1,a)] Gian Andrea Rizzi,[1,2] Davide Barreca,[2,a)] Alberto Gasparotto,[1,2] and Chiara Maccato[1,2]

[1] *Department of Chemical Sciences, Padova University and INSTM, 35131 Padova, Italy*

[2] *CNR-ICMATE and INSTM, Department of Chemical Sciences, Padova University, 35131 Padova, Italy*

(Received day Month year; accepted day Month year; published day Month year)

Materials based on graphitic carbon nitride (gCN) have drawn a great deal of attention as (photo)electrocatalysts triggering the oxygen evolution reaction (OER) in H_2O splitting processes to yield hydrogen fuel. In this work, non-monochromatized Mg Kα radiation (1253.6 eV) was used to acquire photoelectron spectroscopy data on gCN-containing composite systems supported on fluorine-doped tin oxide (FTO). The investigated materials were prepared *via* a straightforward decantation route to yield carbon nitride, followed by functionalization with low amounts of nanostructured co-catalysts (CoO, $CoFe_2O_4$) through radio frequency (RF)-sputtering, and final thermal treatment under an inert atmosphere. Structural and morphological analyses highlighted the formation of composite systems, in which the single constituents, featuring an intimate contact, maintained their chemical identity. This work proposes a data record including both survey scans and high-resolution spectra of C 1s, N 1s, O 1s, Co 2p and Fe 2p core-levels for three representative specimens comprising bare and functionalized graphitic carbon nitride (gCN, gCN-CoO, gCN-$CoFe_2O_4$). The obtained results, discussed in relation to the different chemical environments for the various elements, will be useful as a comparison for further studies in related fields.

Keywords: graphitic carbon nitride; CoO; $CoFe_2O_4$; decantation; RF-sputtering; X-ray photoelectron spectroscopy

Acccession#: 01815, 01816, and 01817

Technique: XPS

Host Material: gCN; gCN-CoO; gCN-$CoFe_2O_4$

Instrument: Perkin-Elmer Physical Electronics, Inc. 5600ci

Major Elements in Spectra: C, N, O, Co, Fe

Minor Elements in Spectra: none

Published Spectra: 15

Spectra in Electronic Record: 15

Spectral Category: comparison

INTRODUCTION

The obtainment of molecular hydrogen (H_2), a strategically appealing energy vector, through photoelectrochemical water splitting activated by solar light, paves the way to large-scale and sustainable energy generation (Refs. 1-3). Nonetheless, one of the main obstacles still hindering economic viability is the kinetically unfavoured oxygen evolution reaction (OER) (Refs. 4, 5), the overall process bottleneck. As a consequence, several efforts have been, and are being, undertaken worldwide for the development of efficient, cheap and environmentally friendly OER catalysts as valuable alternatives to noble metal-based ones, suffering from toxicity, high cost, supply shortage and limited long-term stability (Refs. 4, 6, 7). In this context, graphitic carbon nitride (gCN) has emerged as an amenable candidate thanks to its favourable characteristics, encompassing chemical stability, non-toxicity, suitable band edge positions, and optical band gap enabling Vis light absorption (E_G = 2.7 eV) (Refs. 8-10). To enhance the photoactivity of bare gCN, an attractive option is offered by the design of its nano-organization and by its combination with transition metal oxide co-catalysts (Refs. 11-14). Among the latter, CoO and $CoFe_2O_4$ stand as an appealing choice thanks to their inherent activity in different oxidation reactions, and in fact various reports on their combination with gCN for photocatalytic pollutant degradation (Refs. 9, 10, 15-17) and photoelectrochemical water splitting (Refs. 8, 18, 19) are available in the literature. Nonetheless, only a few works have been focused on the fabrication of supported systems (Refs. 18-21), which offer significant benefits over powdered ones for eventual real-world technological application.

In this widespread context, our group is devoting particular efforts to the design, preparation and characterization of suitably functionalized gCN-based photoelectrocatalysts for both OER (Refs. 22, 23) and water purification from selected pollutants. In particular, in the present study the target materials are prepared by means of a two-step fabrication procedure. First, gCN systems are deposited on fluorine-doped tin oxide (FTO) substrates by a simple decantation procedure. Subsequently, radio frequency (RF)-sputtering is used under mild conditions for the system functionalization with low amounts of CoO and $CoFe_2O_4$ co-catalysts, taking advantage of its inherent infiltration capability to achieve an intimate contact between the system components (Refs. 23, 24). In fact, preliminary results point out to the beneficial role of the resulting nitride-oxide junctions in enhancing OER functional performances and achieving an improved service life, important pre-requisites for practical end-uses.

Within the above scenario, this work presents an XPS data record comprising a detailed analysis of gCN, gCN-CoO and gCN-$CoFe_2O_4$ materials on FTO substrates. The investigation was performed using a standard Mg Kα X-ray source, devoting particular attention to the C 1s, N 1s, O 1s, Co 2p, and Fe 2p photopeaks and to the pertaining spectral features. The obtained data reveal the formation of gCN systems containing a non-negligible amount of uncondensed amino group, that may possibly act as grafting sites for CoO and $CoFe_2O_4$ nanoparticles. The results presented herein may serve as a useful comparison in

[a)] Authors to whom correspondence should be addressed. E-mail: mattia.benedet@phd.unipd.it (M.B.); davide.barreca@unipd.it (D.B.).

the XPS investigation of analogous materials for a variety of applications, as well as a pointer for the synthesis of improved photoelectrocatalysts for the production of solar fuel.

SPECIMEN DESCRIPTION (ACCESSION # 01815)

Host Material: gCN

CAS Registry #: unknown

Host Material Characteristics: homogeneous; solid; polycrystalline; semiconductor; inorganic compound; Thin Film

Chemical Name: graphitic carbon nitride

Source: specimen prepared by decantation of gCN on FTO, followed by thermal treatment in Ar atmosphere at 500°C

Host Composition: C, N, O

Form: Supported thin film

Structure: X-ray diffraction (XRD) revealed the presence of two relatively broad signals at 2θ = 13.1°, associated with the packing of tri-s-triazine units ((100) diffraction plane (Ref. 25), and 2θ = 27.2°, related to the (002) crystallographic planes corresponding to the interplanar stacking of carbon nitride sheets (Ref. 26). Both signals were partially overlapped with the intense reflections of the FTO-coated glass substrate. Field emission-scanning electron microscopy (FE-SEM) analyses (see the inset in figure Accession # **01815-01**) evidenced a granular morphology arising from the even interconnection of gCN aggregates featuring a broad dimensional distribution (500 nm - 4 µm; average deposit thickness = 13 µm).

History & Significance: The carbon nitride powders used as precursor for the target materials were prepared by melamine thermal condensation. Specifically, melamine (99%, Sigma-Aldrich; 2.0 g) was subjected to thermal treatment under Ar in three steps at a fixed heating rate ($2°C \times min^{-1}$) at 100°C (30 min), 400°C (150 min), and 550°C (240 min). As a result, a light-yellow powder was recovered. Subsequently, powders (16.0 mg) were grinded, subsequently suspended in 2-propanol (8.0 mL) and sonicated for 60 min. The resulting suspension was hence transferred into a beaker containing a pre-cleaned FTO-coated glass slide (Sigma-Aldrich®; ≈7 $\Omega \times sq^{-1}$; FTO layer thickness ≈600 nm) on the bottom. After 24 h, the obtained FTO-supported deposit was dried in air for 15 min and then annealed in Ar atmosphere (500°C, 150 min; heating rate = $3°C \times min^{-1}$).

As Received Condition: as grown

Analyzed Region: same as host material

Ex Situ Preparation/Mounting: Sample fixed on a metallic sample holder and introduced into the analysis chamber through a fast entry lock system.

In Situ Preparation: none

Charge Control: No flood gun was used during analysis.

Temp. During Analysis: 298 K

Pressure During Analysis: $<10^{-8}$ Pa

Pre-analysis Beam Exposure: 180 s.

SPECIMEN DESCRIPTION (ACCESSION # 01816)

Host Material: gCN-CoO

CAS Registry #: unknown

Host Material Characteristics: homogeneous; solid; polycrystalline; semiconductor; composite; Thin Film

Chemical Name: graphitic carbon nitride-cobalt(II) oxide

Source: specimen prepared by decantation of gCN on FTO, followed by functionalization with CoO *via* RF-sputtering and thermal treatment in Ar atmosphere at 500°C

Host Composition: C, N, O, Co

Form: Supported nanocomposite thin film

Structure: The specimen XRD pattern did not display any appreciable differences with respect to the one of bare gCN (see the previous sample). The lack of clearly detectable signals ascribable to CoO was mainly traced back to its low amount and high dispersion. FE-SEM analysis (see the inset in figure Accession # **01816-01**) revealed a morphology similar to the previous specimen, although high-resolution micrographs evidenced the presence of globular nanoaggregates related to the metal oxide deposited via RF-sputtering. In fact, transmission electron microscopy (TEM) and selected area electron diffraction (SAED) analyses highlighted the formation of cubic CoO in the form of low-sized nanoparticles (mean diameter = (5±1) nm). Cross-sectional energy dispersive X-ray spectroscopy (EDXS) analyses evidenced that cobalt oxide presence was not limited to the near-surface regions of the deposit, but extended even to the inner ones. This result was related to the porous morphology of carbon nitride, combined with the inherent RF-sputtering infiltration power (Refs. 23, 24).

History & Significance: The preparation of FTO-supported carbon nitride was the same reported for specimen g-CN (see the previous accession). Functionalization with CoO was performed from an Ar plasma (purity = 5.0) using a custom-made two-electrode RF plasmochemical apparatus (ν = 13.56 MHz). Specifically, a cobalt target (Alfa Aesar®; purity = 99.95%) was mounted on the RF-electrode, while FTO-supported gCN was fixed on the grounded one. Basing on previously obtained results (Ref. 24), deposition was carried out for 180 min using the following conditions: growth temperature = 60°C; RF-power = 20 W; Ar flow rate = 10 standard cubic centimeters per minute (sccm); total pressure = 0.3 mbar. The obtained sample was ultimately annealed at 500°C in Ar atmosphere for 150 min (heating rate = 3°C/min).

As Received Condition: as grown

Analyzed Region: same as host material

Ex Situ Preparation/Mounting: Sample fixed on a metallic sample holder and introduced into the analysis chamber through a fast entry lock system.

In Situ Preparation: none

Charge Control: No flood gun was used during analysis.

Temp. During Analysis: 298 K

Pressure During Analysis: $<10^{-8}$ Pa

Pre-analysis Beam Exposure: 180 s.

SPECIMEN DESCRIPTION (ACCESSION # 01817)

Host Material: gCN-$CoFe_2O_4$

CAS Registry #: unknown

Host Material Characteristics: homogeneous; solid; polycrystalline; semiconductor; composite; Thin Film

Chemical Name: graphitic carbon nitride-cobalt ferrite

Source: specimen prepared by decantation of gCN on FTO, followed by functionalization with $CoFe_2O_4$ by RF-sputtering and thermal treatment in Ar atmosphere at 500°C

Host Composition: C, N, O, Co, Fe

Form: Supported nanocomposite thin film

Structure: Specimen characterization by XRD, FE-SEM and EDXS yielded features analogous to those of the gCN-CoO sample as far as the carbon nitride matrix is concerned (see the previous accession). TEM and SAED analyses revealed the presence of crystalline nanoparticles with an average diameter close to 5 nm, whose structure corresponded to spinel-type $CoFe_2O_4$.

History & Significance: The preparation of FTO-supported carbon nitride was carried out under the same conditions reported for the two previous samples. Functionalization with $CoFe_2O_4$ was performed by RF-sputtering using a Co_3O_4-Fe_2O_3 target (Neyco®; purity = 99.9%) using the same plasmochemical reactor and the same experimental settings indicated for gCN-CoO, apart from the sputtering time (195 min). Finally, annealing under Ar was carried out as for the previous sample.

As Received Condition: as grown

Analyzed Region: same as host material

Ex Situ Preparation/Mounting: Sample fixed on a metallic sample holder and introduced into the analysis chamber through a fast entry lock system.

In Situ Preparation: none

Charge Control: No flood gun was used during analysis.

Temp. During Analysis: 298 K

Pressure During Analysis: $<10^{-8}$ Pa

Pre-analysis Beam Exposure: 180 s.

INSTRUMENT DESCRIPTION

Manufacturer and Model: Perkin-Elmer Physical Electronics, Inc. 5600ci

Analyzer Type: spherical sector

Detector: Channeltron

Number of Detector Elements: 16

INSTRUMENT PARAMETERS COMMON TO ALL SPECTRA

■*Spectrometer*

Analyzer Mode: constant pass energy

Throughput ($T=E^N$): N=0

Excitation Source Window: 1.5 micron Al window

Excitation Source: Mg Ka

Source Energy: 1253.6 eV

Source Strength: 200 W

Source Beam Size: > 25000 μm x > 25000 μm

Signal Mode: multichannel direct

■*Geometry*

Incident Angle: 9°

Source-to-Analyzer Angle: 53.8°

Emission Angle: 45°

Specimen Azimuthal Angle: 0°

Acceptance Angle from Analyzer Axis: 0°

Analyzer Angular Acceptance Width: 14° × 14°

■*Ion Gun*

Manufacturer and Model: PHI 04-303 A

Energy: 3000 eV

Current: 0.5 mA/cm2

Current Measurement Method: Faraday cup

Sputtering Species: Ar^+

Spot Size (unrastered): 250 μm

Raster Size: 2000 μm x 2000 μm

Incident Angle: 40 °

Polar Angle: 45 °

Azimuthal Angle: 111 °

Comment: differentially pumped ion gun

DATA ANALYSIS METHOD

Energy Scale Correction: None

Recommended Energy Scale Shift: 0 eV for all specimens

Peak Shape and Background Method: After a Shirley-type background subtraction, BE and full width at half maximum (FWHM) values were determined by least-squares fitting adopting Gaussian/Lorentzian sum functions (typical mixing parameter = 0.2 - 0.3) (Ref. 27).

Quantitation Method: Atomic concentrations were determined by peak area integration, using sensitivity factors provided by PHI V5.4A software.

ACKNOWLEDGMENTS

The authors acknowledge financial support from the National Council of Research (Progetti di Ricerca @CNR - avviso 2020 - ASSIST), Padova University (DOR 2020-2022, P-DiSC#04BIRD2020-UNIPD EUREKA), AMGA Foundation (NYMPHEA project) and INSTM Consortium (INSTM21PDBARMAC-ATENA, INSTM21PDGASPAROTTO-NANO^{MAT}). Many thanks are also due to Dr. Riccardo Lorenzin for his valuable experimental help.

CONFLICT OF INTEREST

The authors have no conflicts to disclose.

DATA AVAILABILITY

The data that support the findings of this study are available within the article and its supplementary material.

REFERENCES

1. X. Han, C. Yu, S. Zhou, C. Zhao, H. Huang, J. Yang, Z. Liu, J. Zhao, and J. Qiu, Adv. Energy Mater. **7**, 1602148 (2017).

2. M. G. Walter, E. L. Warren, J. R. McKone, S. W. Boettcher, Q. Mi, E. A. Santori, and N. S. Lewis, Chem. Rev. **110**, 6446 (2010).
3. J. Zhang, R. García-Rodríguez, P. Cameron, and S. Eslava, Energy Environ. Sci. **11**, 2972 (2018).
4. M. Yu, E. Budiyanto, and H. Tüysüz, Angew. Chem. Int. Ed. **61**, e202103824 (2022).
5. P. Gölitz, M. A. Rowan, and D. J. Smith, ChemCatChem **3**, 4 (2011).
6. P. Guo, Z. Wang, S. Ge, H. Chen, J. Zhang, H. Wang, S. Liu, S. Wei, and X. Lu, ACS Sustainable Chem. Eng. **8**, 4773 (2020).
7. T. Bhowmik, M. K. Kundu, and S. Barman, ACS Appl. Energy Mater. **1**, 1200 (2018).
8. M. Han, H. Wang, S. Zhao, L. Hu, H. Huang, and Y. Liu, Inorg. Chem. Front. **4**, 1691 (2017).
9. S. Huang, Y. Xu, M. Xie, H. Xu, M. He, J. Xia, L. Huang, and H. Li, Colloids Surf., A **478**, 71 (2015).
10. M. Ismael, and M. Wark, FlatChem **32**, 100337 (2022).
11. R. Malik, and V. K. Tomer, Renewable Sustainable Energy Rev. **135**, 110235 (2021).
12. Z. Tian, X. Yang, Y. Chen, H. Huang, J. Hu, and B. Wen, Int. J. Hydrogen Energy **45**, 24792 (2020).
13. H. Zhang, W. Tian, X. Guo, L. Zhou, H. Sun, M. O. Tadé, and S. Wang, ACS Appl. Mater. Interfaces **8**, 35203 (2016).
14. Z. Zhao, Y. Sun, and F. Dong, Nanoscale **7**, 15 (2015).
15. Ö. Görmez, E. Yakar, B. Gözmen, B. Kayan, and A. Khataee, Chemosphere **288**, 132663 (2022).
16. F. Guo, W. Shi, H. Wang, M. Han, H. Li, H. Huang, Y. Liu, and Z. Kang, Catal. Sci. Technol. **7**, 3325 (2017).
17. J. Niu, Y. Xie, H. Luo, Q. Wang, Y. Zhang, and Y. Wang, Chemosphere **218**, 169 (2019).
18. Z. Chen, H. Wang, J. Xu, and J. Liu, Chem. Asian J. **13**, 1539 (2018).
19. Q. Song, J. Li, L. Wang, Y. Qin, L. Pang, and H. Liu, J. Catal. **370**, 176 (2019).
20. P. C. Nagajyothi, K. Yoo, I. Y. Eom, and J. Shim, Ceram. Int. **48**, 11623 (2022).
21. B. Rani, A. K. Nayak, and N. K. Sahu, Diamond Relat. Mater. **120**, 108671 (2021).
22. M. Benedet, A. Gasparotto, G. A. Rizzi, D. Barreca, and C. Maccato, Surf. Sci. Spectra **29**, 024001 (2022).
23. M. Benedet, G. A. Rizzi, A. Gasparotto, O. I. Lebedev, L. Girardi, C. Maccato, and D. Barreca, Chem. Eng. J. **448**, 137645 (2022).
24. C. Maccato, L. Bigiani, L. Girardi, A. Gasparotto, O. I. Lebedev, E. Modin, D. Barreca, and G. A. Rizzi, Adv. Mater. Interfaces **8**, 2100763 (2021).
25. J. H. Thurston, N. M. Hunter, and K. A. Cornell, RSC Adv. **6**, 42240 (2016).
26. F. Fina, S. K. Callear, G. M. Carins, and J. T. S. Irvine, Chem. Mater. **27**, 2612 (2015).
27. V. Jain, M. C. Biesinger, and M. R. Linford, Appl. Surf. Sci. **447**, 548 (2018).
28. J. Wang, and W.-D. Zhang, Electrochim. Acta **71**, 10 (2012).
29. K. Wang, Q. Li, B. Liu, B. Cheng, W. Ho, and J. Yu, Appl. Catal., B **176-177**, 44 (2015).
30. H. Yu, R. Shi, Y. Zhao, T. Bian, Y. Zhao, C. Zhou, G. I. N. Waterhouse, L.-Z. Wu, C.-H. Tung, and T. Zhang, Adv. Mater. **29**, 1605148 (2017).
31. Y. Zhang, Z. Chen, J. Li, Z. Lu, and X. Wang, J. Energy Chem. **54**, 36 (2021).
32. D. Zhang, L. Peng, K. Liu, H. Garcia, C. Sun, and L. Dong, Chem. Eng. J. **381**, 122576 (2020).
33. D. Briggs, and M. P. Seah, *Practical Surface Analysis: Auger and X-ray Photoelectron Spectroscopy* (2nd ed., Wiley, New York, 1990).
34. J. F. Moulder, W. F. Stickle, P. E. Sobol, and K. D. Bomben, *Handbook of X-ray Photoelectron Spectroscopy* (Perkin Elmer Corporation, Eden Prairie, MN, USA, 1992).
35. Q. Liang, Z. Li, Z.-H. Huang, F. Kang, and Q.-H. Yang, Adv. Funct. Mater. **25**, 6885 (2015).
36. F. Hu, W. Luo, C. Liu, H. Dai, X. Xu, Q. Yue, L. Xu, G. Xu, Y. Jian, and X. Peng, Chemosphere **274**, 129783 (2021).
37. J. Fu, B. Zhu, C. Jiang, B. Cheng, W. You, and J. Yu, Small **13**, 1603938 (2017).
38. Q. Zheng, Y. Xu, Y. Wan, J. Wu, X. Hu, and X. Yao, J. Nanopart. Res. **22**, 301 (2020).
39. Y. Xiao, G. Tian, W. Li, Y. Xie, B. Jiang, C. Tian, D. Zhao, and H. Fu, J. Am. Chem. Soc. **141**, 2508 (2019).
40. D. Barreca, A. Gasparotto, O. I. Lebedev, C. Maccato, A. Pozza, E. Tondello, S. Turner, and G. Van Tendeloo, CrystEngComm **12**, 2185 (2010).
41. Z. Wu, P. Li, Q. Qin, Z. Li, and X. Liu, Carbon **139**, 35 (2018).
42. J. Chen, D. Zhao, Z. Diao, M. Wang, and S. Shen, Sci. Bull. **61**, 292 (2016).
43. B. Palanivel, M. Lallimathi, B. Arjunkumar, M. Shkir, T. Alshahrani, K. S. Al-Namshah, M. S. Hamdy, S. Shanavas, M. Venkatachalam, and G. Ramalingam, J. Environ. Chem. Eng. **9**, 104698 (2021).
44. G. Wang, Y. Ma, Z. Wei, and M. Qi, Chem. Eng. J. **289**, 150 (2016).
45. F. Urbain, R. Du, P. Tang, V. Smirnov, T. Andreu, F. Finger, N. Jimenez Divins, J. Llorca, J. Arbiol, A. Cabot, and J. R. Morante, Appl. Catal., B **259**, 118055 (2019).

SPECTRAL FEATURES TABLE

Spectrum ID #	Element/ Transition	Peak Energy (eV)	Peak Width FWHM (eV)	Peak Area (eV x cts/s)	Sensitivity Factor	Concentration (at. %)	Peak Assignment
01815-02[a]	C 1s	284.8	1.8	4739.1	0.296	11.4	Adventitious surface contamination
01815-02[a]	C 1s	286.2	2.1	3145.8	0.296	7.5	C in C-NH_x (x=1,2) groups on the edges of heptazinic rings
01815-02[a]	C 1s	288.3	1.8	12542.2	0.296	30.0	C in N-C=N moieties of gCN aromatic rings and adsorbed carbonates
01815-03[b]	N 1s	398.6	1.7	20188.6	0.477	30.0	Two-coordinated C=N-C N atoms in gCN
01815-03[b]	N 1s	399.9	2.0	7123.5	0.477	10.6	Tri-coordinated N atoms [N-$(C)_3$] in the gCN structure
01815-03[b]	N 1s	401.1	2.1	2747.2	0.477	4.1	N in C-NH_x (x=1,2) groups on the edges of heptazinic rings
01815-03[b]	N 1s	404.2	2.6	1884.7	0.477	2.8	π-electrons excitations in heptazine rings
01815-04	O 1s	531.9	2.9	3575.0	0.711	3.6	-OH groups chemisorbed on nitrogen vacancies and adsorbed carbonates
01816-02[a]	C 1s	284.8	1.9	4323.6	0.296	11.3	Adventitious surface contamination
01816-02[a]	C 1s	286.3	2.2	2570.3	0.296	6.7	C in C-NH_x (x=1,2) groups on the edges of heptazinic rings
01816-02[a]	C 1s	288.3	2.0	10128.1	0.296	26.4	C in N-C=N moieties of gCN aromatic rings and adsorbed carbonates
01816-03[b]	N 1s	398.6	1.7	14521.4	0.477	23.5	Two-coordinated C=N-C N atoms in gCN
01816-03[b]	N 1s	399.8	2.1	6734.2	0.477	10.9	Tri-coordinated N atoms [N-$(C)_3$] in the gCN structure
01816-03[b]	N 1s	401.0	1.9	2326.4	0.477	3.8	N in C-NH_x (x=1,2) groups on the edges of heptazinic rings
01816-03[b]	N 1s	404.2	2.9	906.1	0.477	1.5	π-electrons excitations in heptazine rings
01816-04[c]	O 1s	529.9	2.1	2368.9	0.711	2.6	Lattice oxygen in CoO
01816-04[c]	O 1s	531.9	2.6	9075.1	0.711	9.9	-OH groups chemisorbed on nitrogen vacancies and adsorbed carbonates
01816-05[d]	Co 2p	…	…	16262.0	3.590	3.5	Co(II) in CoO
01816-05	Co $2p_{3/2}$	781.1	3.6	…	…	…	Co(II) in CoO
01816-05	Co $2p_{1/2}$	796.7	3.7	…	…	…	Co(II) in CoO
01817-02[a]	C 1s	284.8	1.8	5090.2	0.296	13.0	Adventitious surface contamination
01817-02[a]	C 1s	286.3	2.0	2589.1	0.296	6.6	C in C-NH_x (x=1,2) groups on the edges of heptazinic rings
01817-02[a]	C 1s	288.2	2.0	9933.7	0.296	25.4	C in N-C=N moieties of gCN aromatic rings and adsorbed carbonates
01817-03[b]	N 1s	398.6	1.7	13145.9	0.477	20.8	Two-coordinated C=N-C N atoms in gCN
01817-03[b]	N 1s	399.8	2.1	6248.2	0.477	9.9	Tri-coordinated N atoms [N-$(C)_3$] in the gCN structure
01817-03[b]	N 1s	401.0	1.9	2172.3	0.477	3.4	N in C-NH_x (x=1,2) groups on the edges of heptazinic rings
01817-03[b]	N 1s	404.2	2.9	828.6	0.477	1.3	π-electrons excitations in heptazine rings
01817-04[c]	O 1s	529.9	2.1	3009.1	0.711	3.2	Lattice oxygen in $CoFe_2O_4$
01817-04[c]	O 1s	531.8	2.5	8218.9	0.711	8.7	-OH groups chemisorbed on nitrogen vacancies and adsorbed carbonates
01817-05[d]	Co 2p	…	…	12006.0	3.590	2.5	Co(II) in $CoFe_2O_4$
01817-05	Co $2p_{3/2}$	781.3	3.5	…	…	…	Co(II) in $CoFe_2O_4$

01817-06	Co $2p_{1/2}$	796.8	3.7	…	…	…	Co(II) in $CoFe_2O_4$
01817-06[e]	Fe 2p	...		19513.0	2.957	5.1	Fe(III) in $CoFe_2O_4$
01817-06	Fe $2p_{3/2}$	710.6	3.6	…	…	…	Fe(III) in $CoFe_2O_4$
01817-06	Fe $2p_{1/2}$	723.9	3.6	…	…	…	Fe(III) in $CoFe_2O_4$

[a] The sensitivity factor is referred to the whole C 1s signal.
[b] The sensitivity factor is referred to the whole N 1s signal.
[c] The sensitivity factor is referred to the whole O 1s signal.
[d] The sensitivity factor, peak area, and concentration are referred to the whole Co 2p signal.
[e] The sensitivity factor, peak area, and concentration are referred to the whole Fe 2p signal.

Footnote to Spectra 01815-01, 01816-01 and 01817-01: For all specimens, wide-scan spectra were dominated by carbon and nitrogen signals, as expected. For functionalized samples, the presence of cobalt (gCN-CoO) and cobalt + iron (gCN-$CoFe_2O_4$) photoelectron peaks was in line with the occurrence of cobalt(II) oxide and cobalt ferrite, respectively, as discussed in more detail below.

Footnote to Spectra 01815-02, 01816-02 and 01817-02: For all the investigated samples, three components contributed to the C 1s signal: **i**) adventitious carbon contamination due to air exposure/sample manipulation prior to analysis (BE = 284.8 eV) (Refs. 28, 29); **ii**) C-NH_x (x = 1, 2) moieties located on gCN heptazine ring edges (average BE = 286.3 eV) (Refs. 30, 31); **iii**), the predominant one, due to N-C=N carbon atoms in gCN aromatic rings (average BE = 288.3 eV) (Refs. 8, 17, 28, 32). Nonetheless, a minor contribution to the latter band by adsorbed carbonates resulting from air exposure, yielding a signal with a very close BE value (Refs. 33, 34), was also likely present.

Footnote to Spectra 01815-03, 01816-03 and 01817-03: The N 1s photopeak could be deconvoluted by means of four different contributing bands. The main one, located at BE = 398.6 eV, was ascribed to two-coordinated C=N-C nitrogen atoms in gCN (Refs. 31, 35, 36). The second one, with an average BE of 399.8 eV, was related to tri-coordinated N-$(C)_3$ N atoms in carbon nitride (Refs. 28, 30, 35, 37). The signal at a mean BE of 401.0 eV could be attributed to amino groups (NH_x , with x = 1, 2) in the heptazine framework (average BE = 401.0 eV) (Refs. 29, 36-38), and the last weaker band (BE = 404.2 eV) was due to π-electrons excitations in heptazine rings (Refs. 8, 29, 32, 35). Defects arising from the occurrence of -NH_x moieties can act as capturing sites, suppressing recombination of photo-generated electron-hole pairs, with a positive influence on photoelectrocatalytic activity (Refs. 30, 39).
The absence of any significant spectral variation after functionalization with CoO and $CoFe_2O_4$ indicates that the adopted RF-sputtering procedure is mild enough to avoid any alteration of the pristine gCN chemical features.

Footnote to Spectra 01815-04, 01816-04 and 01817-04: As concerns bare carbon nitride (gCN), the O 1s peak was characterized by a single component centered at BE= 531.9 eV, ascribable to -OH groups chemisorbed on nitrogen vacancies (Refs. 10, 22, 23, 37), and to a possible minor contribution from adsorbed carbonate species (Ref. 34). For functionalized specimens (gCN-CoO and gCN-$CoFe_2O_4$), the O 1s signal presented also an additional band at BE = 529.9 eV related to lattice oxygen in CoO and $CoFe_2O_4$ (Ref. 10, 16, 36, 40, 41). Nevertheless, the signal from -OH groups was always the predominant one, suggesting thus the formation of highly defective systems.

Footnote to Spectra 01816-05 and 01817-05: For both functionalized specimens, the Co 2p photoelectron peaks possessed qualitatively similar spectral features and were characterized by net shake-up satellites at BEs ≈ 5.5 eV higher than the principal spin-orbit components, a finger print for the presence of Co(II) centers (Refs. 18, 32, 42, 43). For sample gCN-CoO, the signal energy location [BE(Co $2p_{3/2}$) = 781.1 eV; spin-orbit splitting (SOS) = 15.6 eV] was in agreement with the presence of cobalt(II) oxide (Refs. 8, 10, 16, 17, 32). As far as gCN-$CoFe_2O_4$ is concerned, the Co 2p position underwent an upward shift of +0.2 eV. The BE(Co $2p_{3/2}$) value of 781.3 eV (SOS = 15.5 eV) was in line with that reported for $CoFe_2O_4$-containing systems (Refs. 15, 38, 44, 45), in accordance with the outcomes of TEM and SAED analyses. The lack of signals centered at ≈778.0 eV indicated the absence of Co metal impurities (Refs. 32, 40).

Footnote to Spectrum 01817-06: At variance with Co 2p peaks, the Fe 2p signal for gCN-$CoFe_2O_4$ was free from shake-up satellites. The energy position [BE(Fe $2p_{3/2}$) = 710.6 eV; SOS = 13.3 eV] was in agreement with that previously reported for MFe_2O_4 materials (M = Mg, Co) (Refs. 9, 15, 36, 42-44).

ANALYZER CALIBRATION TABLE

Spectrum ID #	Element/ Transition	Peak Energy (eV)	Peak Width FWHM (eV)	Peak Area (eV x cts/s)	Sensitivity Factor	Concentration (at. %)	Peak Assignment
…[a]	Au $4f_{7/2}$	84.0	1.4	186403	...	...	Au(0)
…[a]	Cu $2p_{3/2}$	932.7	1.6	86973	...	...	Cu(0)

[a] The peak was acquired after Ar^+ erosion.

GUIDE TO FIGURES

Spectrum (Accession) #	Spectral Region	Voltage Shift*	Multiplier	Baseline	Comment #
01815-01	Survey	0	1	0	…
01815-02	C 1s	0	1	0	…
01815-03	N 1s	0	1	0	…
01815-04	O 1s	0	1	0	…
01816-01	Survey	0	1	0	…
01816-02	C 1s	0	1	0	…
01816-03	N 1s	0	1	0	…
01816-04	O 1s	0	1	0	…
01816-05	Co 2p	0	1	0	…
01817-01	Survey	0	1	0	…
01817-02	C 1s	0	1	0	…
01817-03	N 1s	0	1	0	…
01817-04	O 1s	0	1	0	…
01817-05	Co 2p	0	1	0	…
01817-06	Fe 2p	0	1	0	…

* Voltage shift of the archived (as measured) spectrum relative to the printed figure. The figure reflects the recommended energy scale correction due to a calibration correction, sample charging, flood gun, or other phenomena.

Surf. Sci. Spectra 30, 014004 (2023); https://doi.org/10.1116/6.0002280

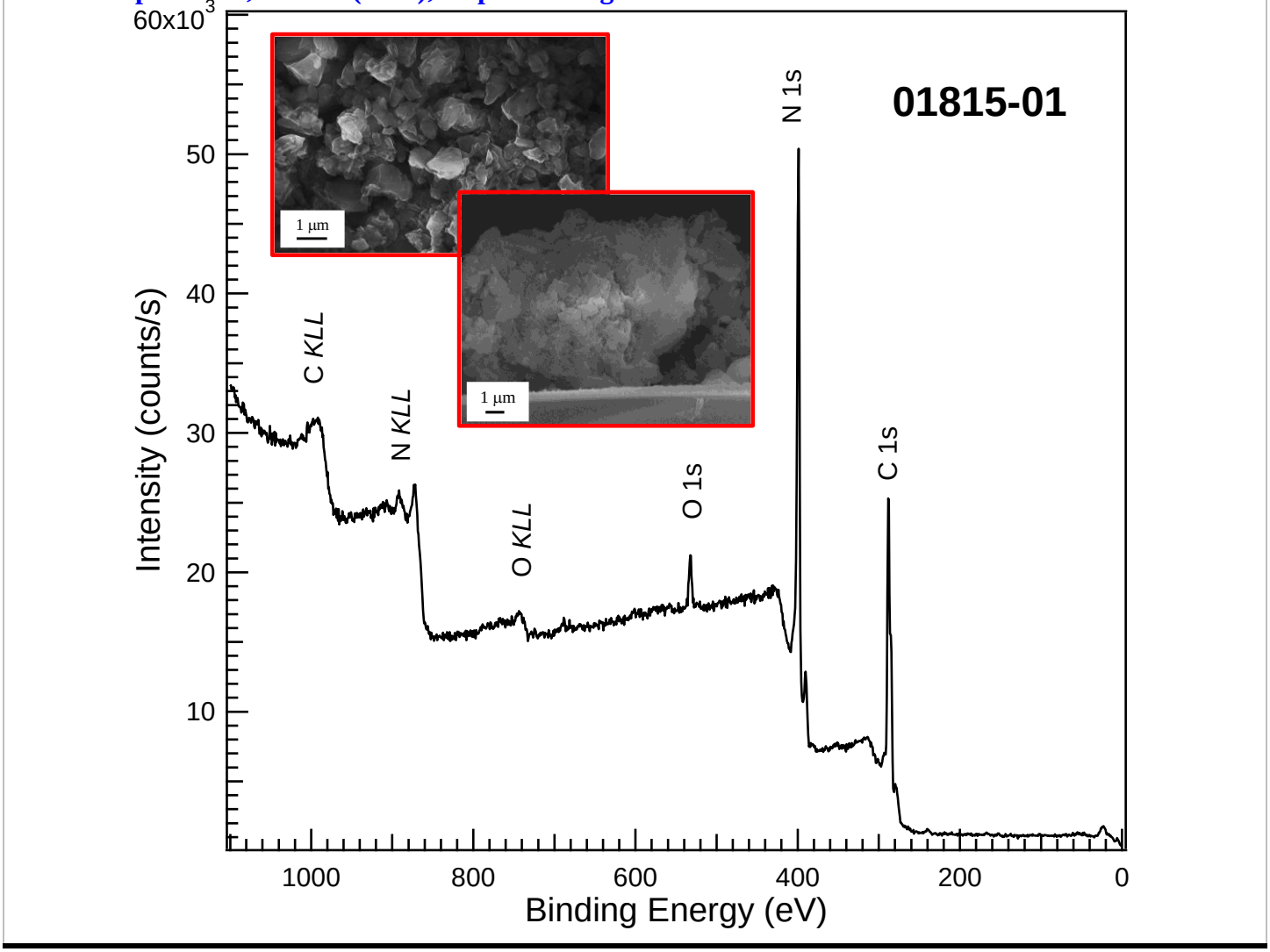

Publish in *Surface Science Spectra*: Yes ☒ No ☐

Accession #	01815-01
Host Material	gCN
Technique	XPS
Spectral Region	survey
Instrument	Perkin-Elmer Physical Electronics, Inc. 5600ci
Excitation Source	Mg Ka
Source Energy	1253.6 eV
Source Strength	200 W
Source Size	>25 mm x >25 mm
Analyzer Type	spherical sector analyzer
Incident Angle	9 ˚
Emission Angle	45 ˚
Analyzer Pass Energy	187.85 eV
Analyzer Resolution	1.9 eV
Total Signal Accumulation Time	577.9 s
Total Elapsed Time	635.7 s
Number of Scans	21
Effective Detector Width	1.9 eV

Surf. Sci. Spectra 30, 014004 (2023); https://doi.org/10.1116/6.0002280

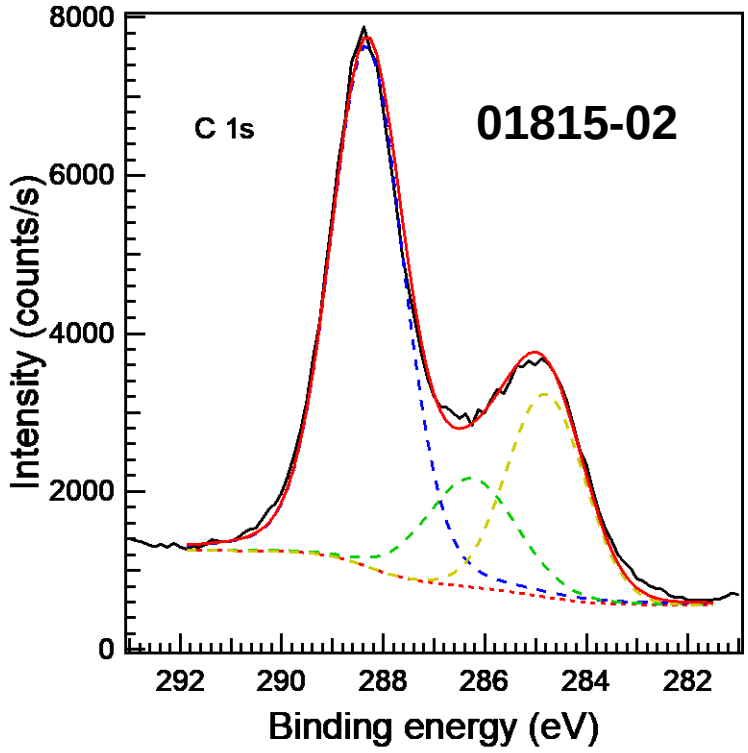

Publish in *SSS*: Yes X No ☐

- **Accession #: 01815-02**
- **Host Material:** gCN
- **Technique:** XPS
- **Spectral Region:** C 1s

Instrument: Perkin-Elmer Physical Electronics, Inc. 5600ci
Excitation Source: Mg Ka
Source Energy: 1253.6 eV
Source Strength: 200 W
Source Size: >25 mm x >25 mm
Analyzer Type: spherical sector
Incident Angle: 9 °
Emission Angle: 45 °
Analyzer Pass Energy 58.7 eV
Analyzer Resolution: 0.6 eV
Total Signal Accumulation Time: 277.5 s
Total Elapsed Time: 305.3 s
Number of Scans: 30
Effective Detector Width: 0.6 eV

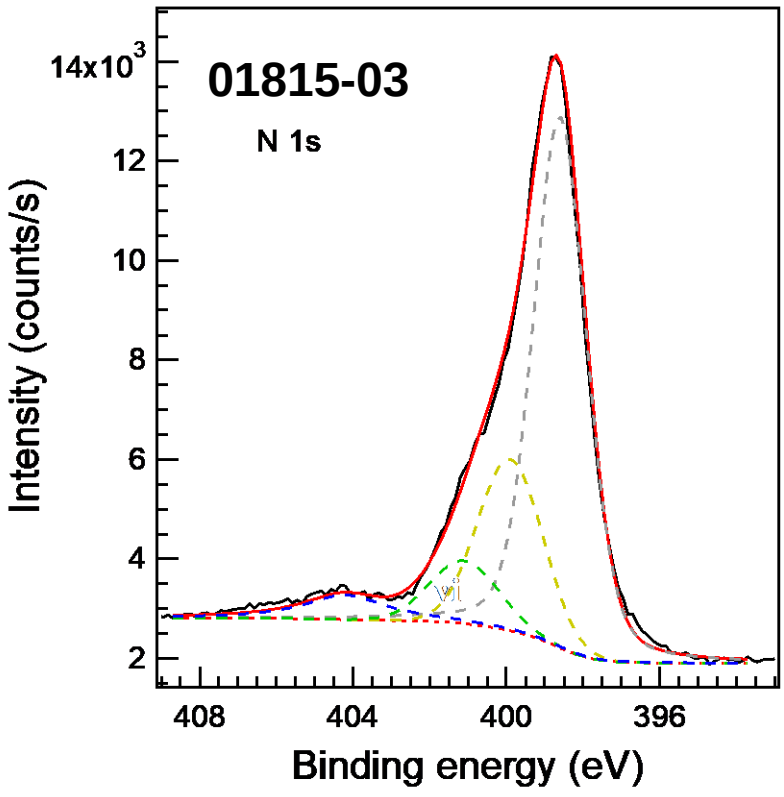

Publish in *SSS*: Yes X No ☐

- **Accession #: 01815-03**
- **Host Material:** gCN
- **Technique:** XPS
- **Spectral Region:** N 1s

Instrument: Perkin-Elmer Physical Electronics, Inc. 5600ci
Excitation Source: Mg Ka
Source Energy: 1253.6 eV
Source Strength: 200 W
Source Size: >25 mm x >25 mm
Analyzer Type: spherical sector
Incident Angle: 9 °
Emission Angle: 45 °
Analyzer Pass Energy 58.7 eV
Analyzer Resolution: 0.6 eV
Total Signal Accumulation Time: 301.5 s
Total Elapsed Time: 331.7 s
Number of Scans: 30
Effective Detector Width: 0.6 eV

Surf. Sci. Spectra 30, 014004 (2023); https://doi.org/10.1116/6.0002280

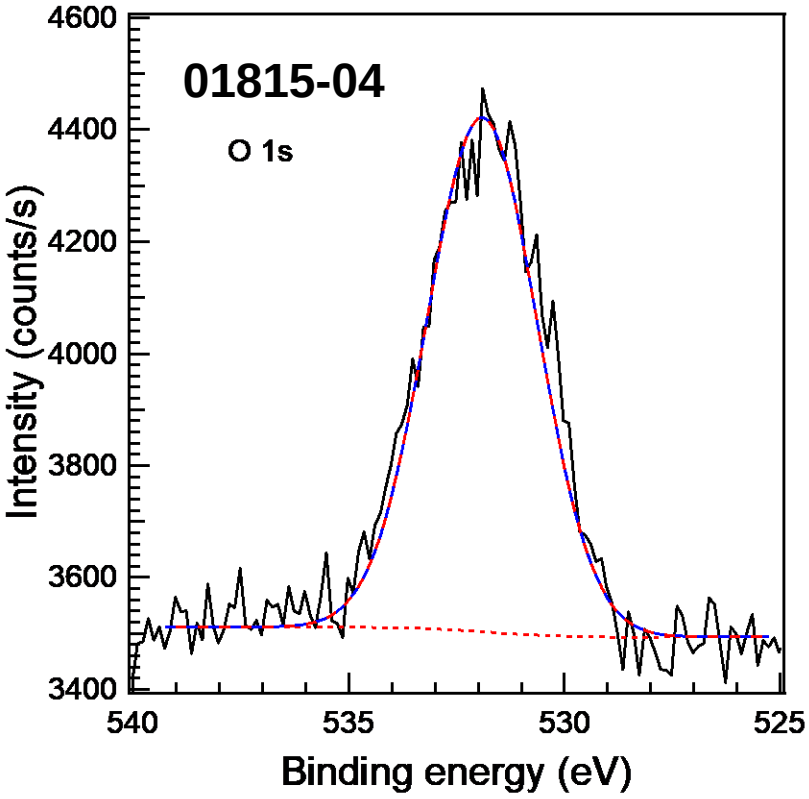

Publish in *SSS*: Yes X No ☐

- **Accession #: 01815-04**
- **Host Material:** gCN
- **Technique:** XPS
- **Spectral Region:** O 1s

Instrument: Perkin-Elmer Physical Electronics, Inc. 5600ci
Excitation Source: Mg Ka
Source Energy: 1253.6 eV
Source Strength: 200 W
Source Size: >25 mm x >25 mm
Analyzer Type: spherical sector
Incident Angle: 9 °
Emission Angle: 45 °
Analyzer Pass Energy 58.7 eV
Analyzer Resolution: 0.6 eV
Total Signal Accumulation Time: 354.2 s
Total Elapsed Time: 389.6 s
Number of Scans: 44
Effective Detector Width: 0.6 eV

Surf. Sci. Spectra 30, 014004 (2023); https://doi.org/10.1116/6.0002280

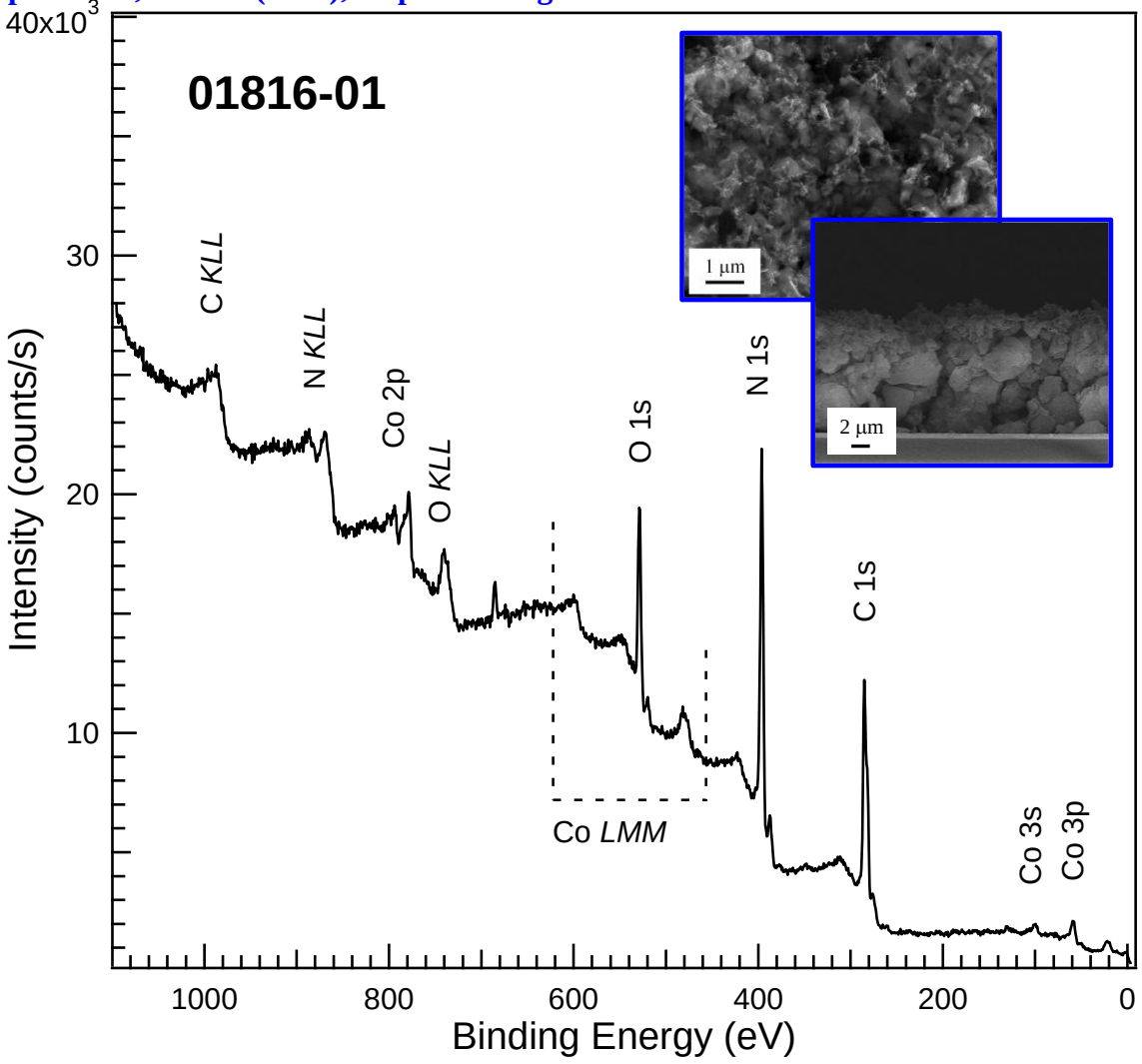

Publish in *Surface Science Spectra*: Yes ☒ No ☐

Accession #	01816-01
Host Material	gCN-CoO
Technique	XPS
Spectral Region	survey
Instrument	Perkin-Elmer Physical Electronics, Inc. 5600ci
Excitation Source	Mg Ka
Source Energy	1253.6 eV
Source Strength	200 W
Source Size	>25 mm x >25 mm
Analyzer Type	spherical sector analyzer
Incident Angle	9 ˚
Emission Angle	45 ˚
Analyzer Pass Energy	187.85 eV
Analyzer Resolution	1.9 eV
Total Signal Accumulation Time	963.2 s
Total Elapsed Time	1059.5 s
Number of Scans	35
Effective Detector Width	1.9 eV

Surf. Sci. Spectra 30, 014004 (2023); https://doi.org/10.1116/6.0002280

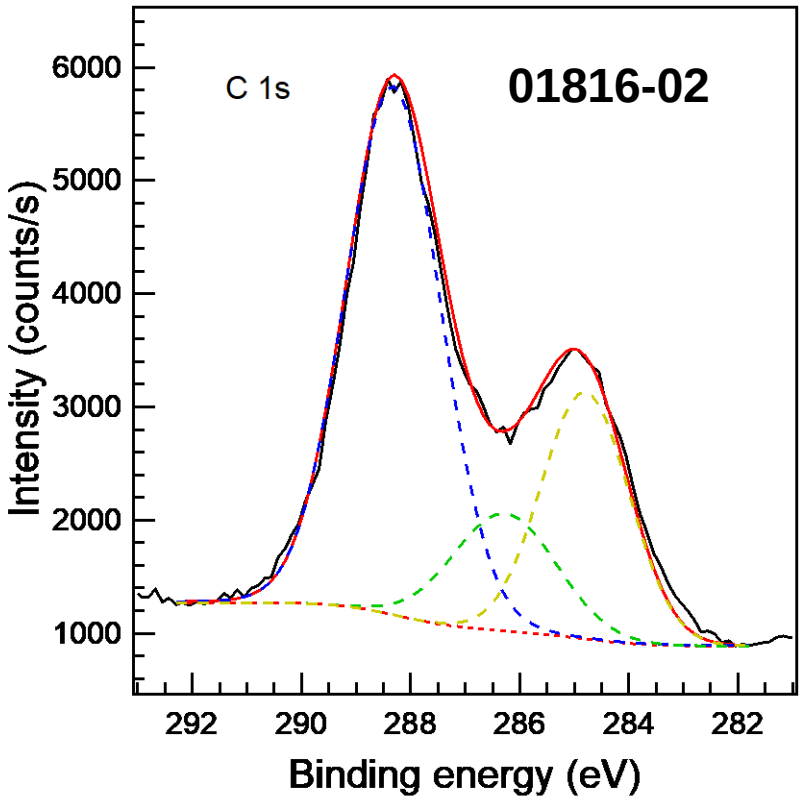

Publish in *SSS*: Yes ☒ No ☐

- **Accession #: 01816-02**
- **Host Material:** gCN-CoO
- **Technique:** XPS
- **Spectral Region:** C 1s

Instrument: Perkin-Elmer Physical Electronics, Inc. 5600ci
Excitation Source: Mg Ka
Source Energy: 1253.6 eV
Source Strength: 200 W
Source Size: >25 mm x >25 mm
Analyzer Type: spherical sector
Incident Angle: 9 °
Emission Angle: 45 °
Analyzer Pass Energy 58.7 eV
Analyzer Resolution: 0.6 eV
Total Signal Accumulation Time: 212.4 s
Total Elapsed Time: 233.6 s

Number of Scans: 24

Effective Detector Width: 0.6 eV

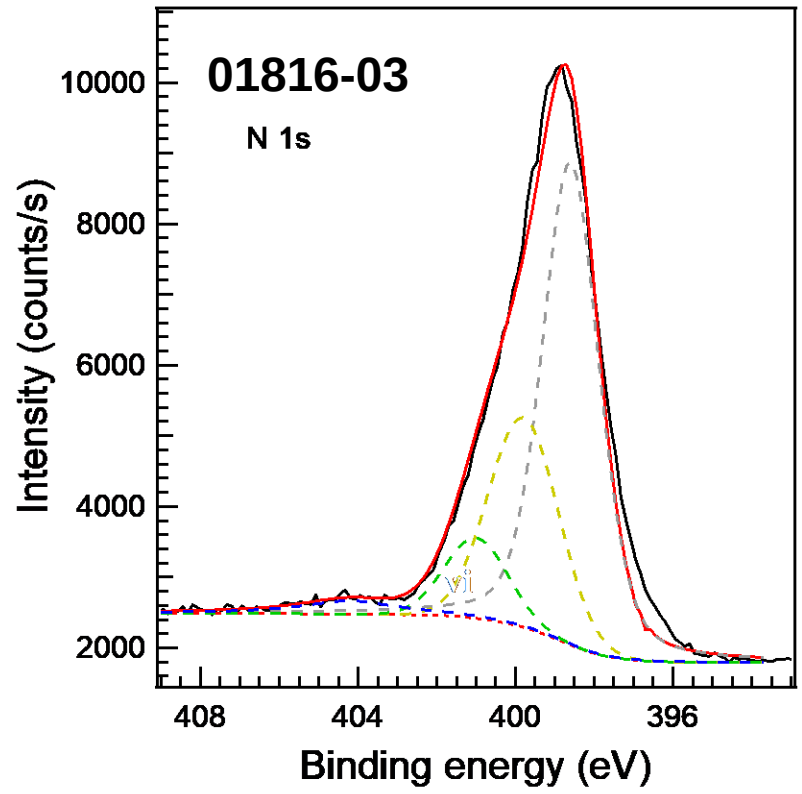

Publish in *SSS*: Yes ☒ No ☐

- **Accession #: 01816-03**
- **Host Material:** gCN-CoO
- **Technique:** XPS
- **Spectral Region:** N 1s

Instrument: Perkin-Elmer Physical Electronics, Inc. 5600ci
Excitation Source: Mg Ka
Source Energy: 1253.6 eV
Source Strength: 200 W
Source Size: >25 mm x >25 mm
Analyzer Type: spherical sector
Incident Angle: 9 °
Emission Angle: 45 °
Analyzer Pass Energy 58.7 eV
Analyzer Resolution: 0.6 eV
Total Signal Accumulation Time: 325.4 s
Total Elapsed Time: 357.9 s

Number of Scans: 27

Effective Detector Width: 0.6 eV

Surf. Sci. Spectra 30, 014004 (2023); https://doi.org/10.1116/6.0002280

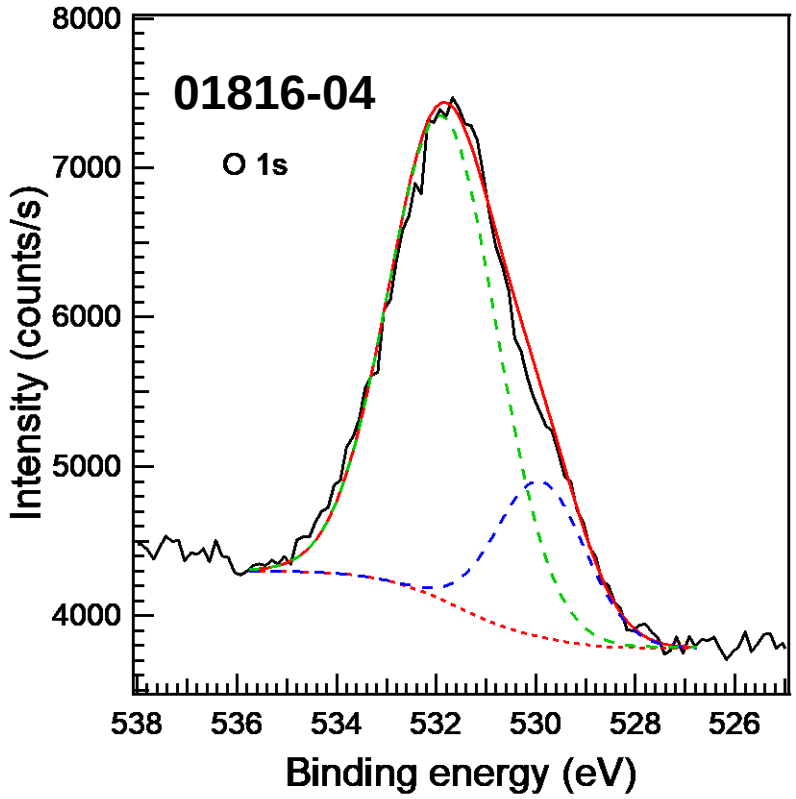

Publish in *SSS*: Yes ☒ No ☐

- **Accession #: 01816-04**
- **Host Material:** gCN-CoO
- **Technique:** XPS
- **Spectral Region:** O 1s

Instrument: Perkin-Elmer Physical Electronics, Inc. 5600ci
Excitation Source: Mg Ka
Source Energy: 1253.6 eV
Source Strength: 200 W
Source Size: >25 mm x >25 mm
Analyzer Type: spherical sector
Incident Angle: 9 °
Emission Angle: 45 °
Analyzer Pass Energy 58.7 eV
Analyzer Resolution: 0.6 eV
Total Signal Accumulation Time: 241.5 s
Total Elapsed Time: 265.7 s

Number of Scans: 30

Effective Detector Width: 0.6 eV

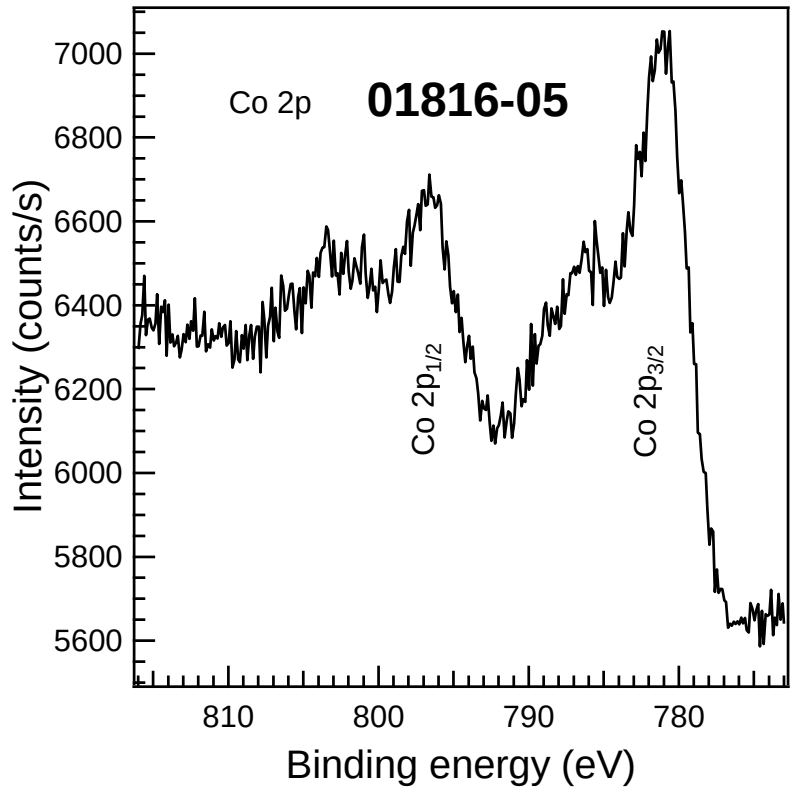

Publish in *SSS*: Yes ☒ No ☐

- **Accession #: 01816-05**
- **Host Material:** gCN-CoO
- **Technique:** XPS
- **Spectral Region:** Co 2p

Instrument: Perkin-Elmer Physical Electronics, Inc. 5600ci
Excitation Source: Mg Ka
Source Energy: 1253.6 eV
Source Strength: 200 W
Source Size: >25 mm x >25 mm
Analyzer Type: spherical sector
Incident Angle: 9 °
Emission Angle: 45 °
Analyzer Pass Energy 58.7 eV
Analyzer Resolution: 0.6 eV
Total Signal Accumulation Time: 1593.8 s
Total Elapsed Time: 1753.2 s

Number of Scans: 75

Effective Detector Width: 0.6 eV

Surf. Sci. Spectra 30, 014004 (2023); https://doi.org/10.1116/6.0002280

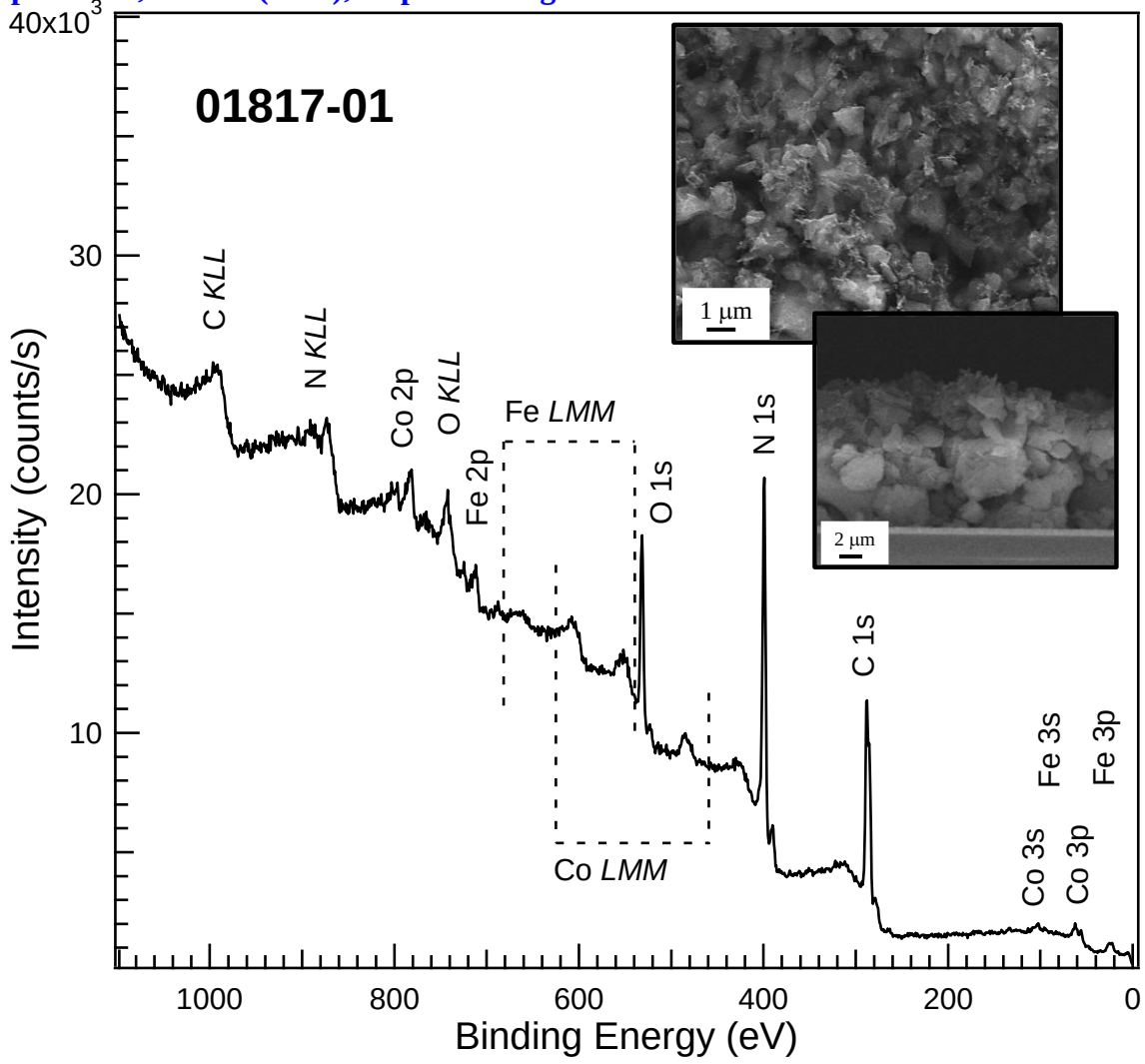

Publish in *Surface Science Spectra*: Yes ☒ No ☐

Accession #	01817-01
Host Material	gCN-$CoFe_2O_4$
Technique	XPS
Spectral Region	survey
Instrument	Perkin-Elmer Physical Electronics, Inc. 5600ci
Excitation Source	Mg Ka
Source Energy	1253.6 eV
Source Strength	200 W
Source Size	>25 mm x >25 mm
Analyzer Type	spherical sector analyzer
Incident Angle	9 ˚
Emission Angle	45 ˚
Analyzer Pass Energy	187.85 eV
Analyzer Resolution	1.9 eV
Total Signal Accumulation Time	908.2 s
Total Elapsed Time	999.0 s
Number of Scans	33
Effective Detector Width	1.9 eV

Surf. Sci. Spectra 30, 014004 (2023); https://doi.org/10.1116/6.0002280

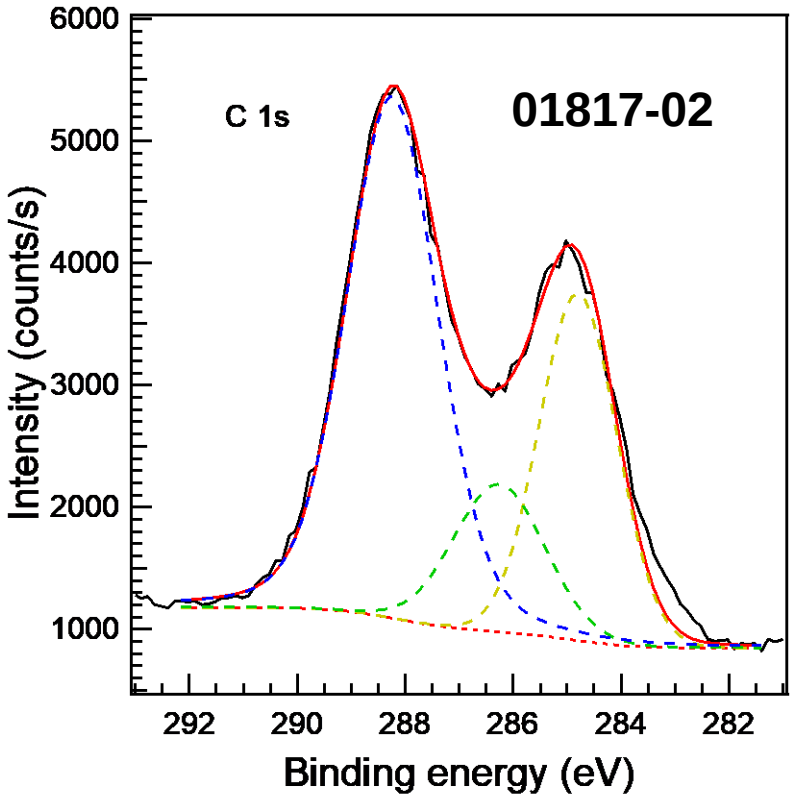

Publish in *SSS*: Yes X No ☐

- **Accession #: 01817-02**
- **Host Material:** gCN-$CoFe_2O_4$
- **Technique:** XPS
- **Spectral Region:** C 1s

Instrument: Perkin-Elmer Physical Electronics, Inc. 5600ci
Excitation Source: Mg Ka
Source Energy: 1253.6 eV
Source Strength: 200 W
Source Size: >25 mm x >25 mm
Analyzer Type: spherical sector
Incident Angle: 9 °
Emission Angle: 45 °
Analyzer Pass Energy 58.7 eV
Analyzer Resolution: 0.6 eV
Total Signal Accumulation Time: 221.3 s
Total Elapsed Time: 243.4 s

Number of Scans: 25

Effective Detector Width: 0.6 eV

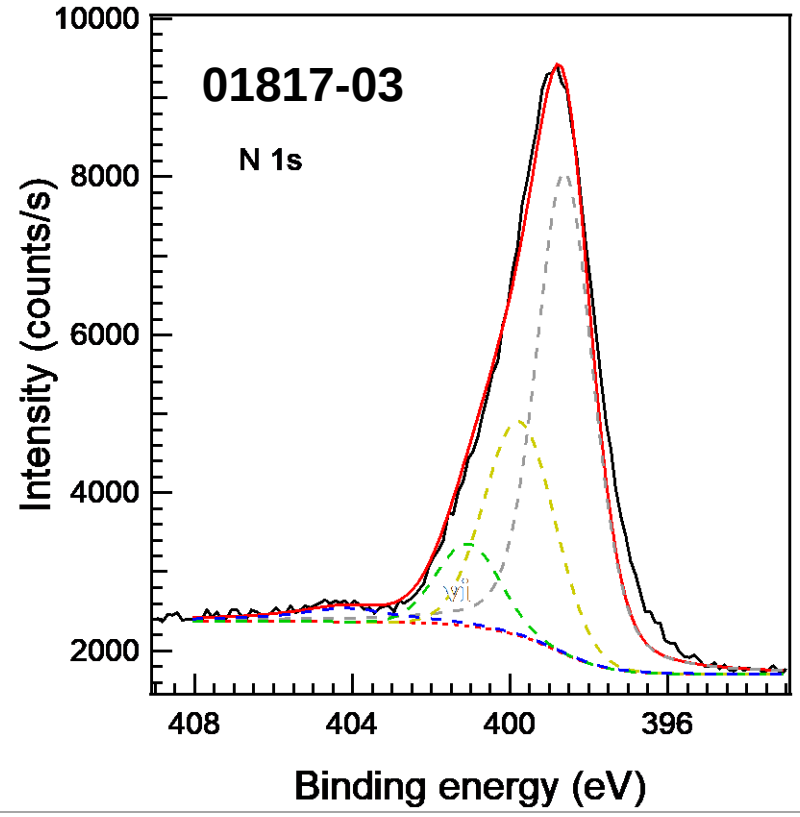

Publish in *SSS*: Yes X No ☐

- **Accession #: 01817-03**
- **Host Material:** gCN-$CoFe_2O_4$
- **Technique:** XPS
- **Spectral Region:** N 1s

Instrument: Perkin-Elmer Physical Electronics, Inc. 5600ci
Excitation Source: Mg Ka
Source Energy: 1253.6 eV
Source Strength: 200 W
Source Size: >25 mm x >25 mm
Analyzer Type: spherical sector
Incident Angle: 9 °
Emission Angle: 45 °
Analyzer Pass Energy 58.7 eV
Analyzer Resolution: 0.6 eV
Total Signal Accumulation Time: 325.4 s
Total Elapsed Time: 357.9 s

Number of Scans: 27

Effective Detector Width: 0.6 eV

Surf. Sci. Spectra 30, 014004 (2023); https://doi.org/10.1116/6.0002280

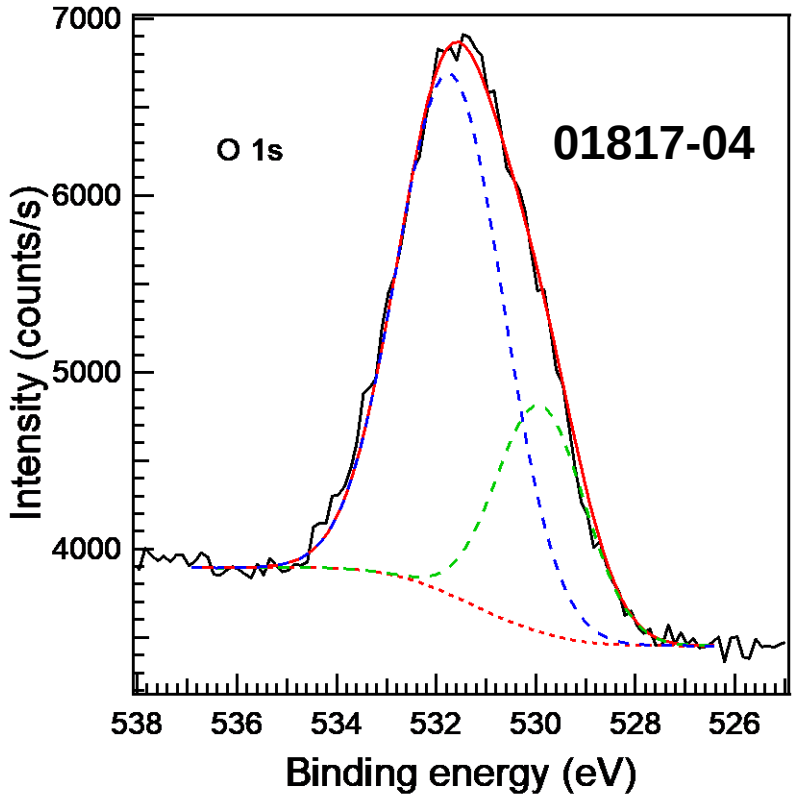

Publish in *SSS*: Yes ☒ No ☐

- **Accession #: 01817-04**
- **Host Material:** $gCN\text{-}CoFe_2O_4$
- **Technique:** XPS
- **Spectral Region:** O 1s

Instrument: Perkin-Elmer Physical Electronics, Inc. 5600ci
Excitation Source: Mg Ka
Source Energy: 1253.6 eV
Source Strength: 200 W
Source Size: >25 mm x >25 mm
Analyzer Type: spherical sector
Incident Angle: 9 °
Emission Angle: 45 °
Analyzer Pass Energy 58.7 eV
Analyzer Resolution: 0.6 eV
Total Signal Accumulation Time: 257.6 s
Total Elapsed Time: 283.4 s

Number of Scans: 32

Effective Detector Width: 0.6 eV

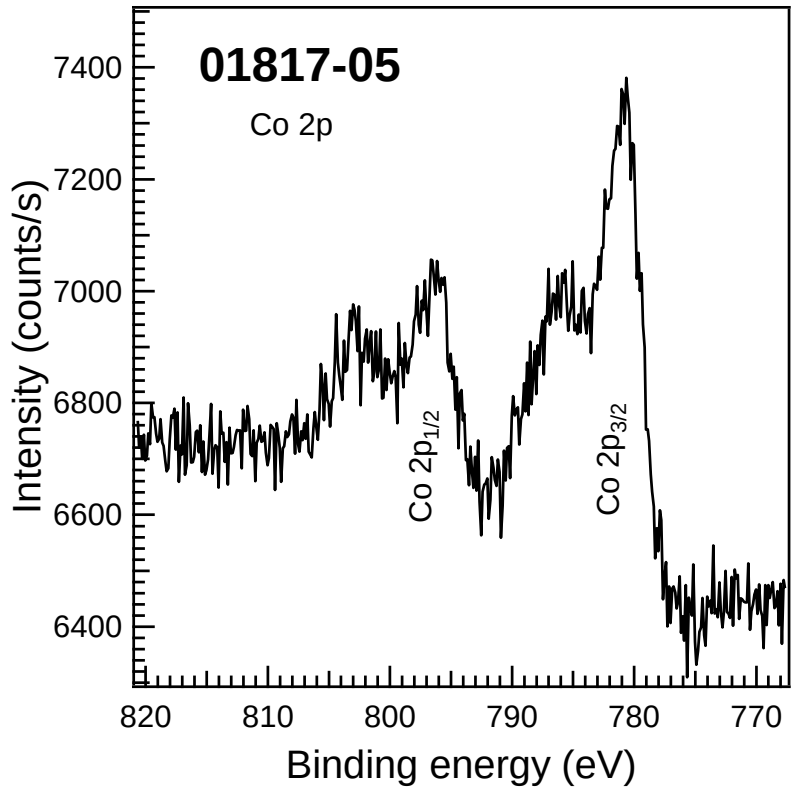

Publish in *SSS*: Yes ☒ No ☐

- **Accession #: 01817-05**
- **Host Material:** $gCN\text{-}CoFe_2O_4$
- **Technique:** XPS
- **Spectral Region:** Co 2p

Instrument: Perkin-Elmer Physical Electronics, Inc. 5600ci
Excitation Source: Mg Ka
Source Energy: 1253.6 eV
Source Strength: 200 W
Source Size: >25 mm x >25 mm
Analyzer Type: spherical sector
Incident Angle: 9 °
Emission Angle: 45 °
Analyzer Pass Energy 58.7 eV
Analyzer Resolution: 0.6 eV
Total Signal Accumulation Time: 1700.0 s
Total Elapsed Time: 1870.0 s

Number of Scans: 80

Effective Detector Width: 0.6 eV

Surf. Sci. Spectra 30, 014004 (2023); https://doi.org/10.1116/6.0002280

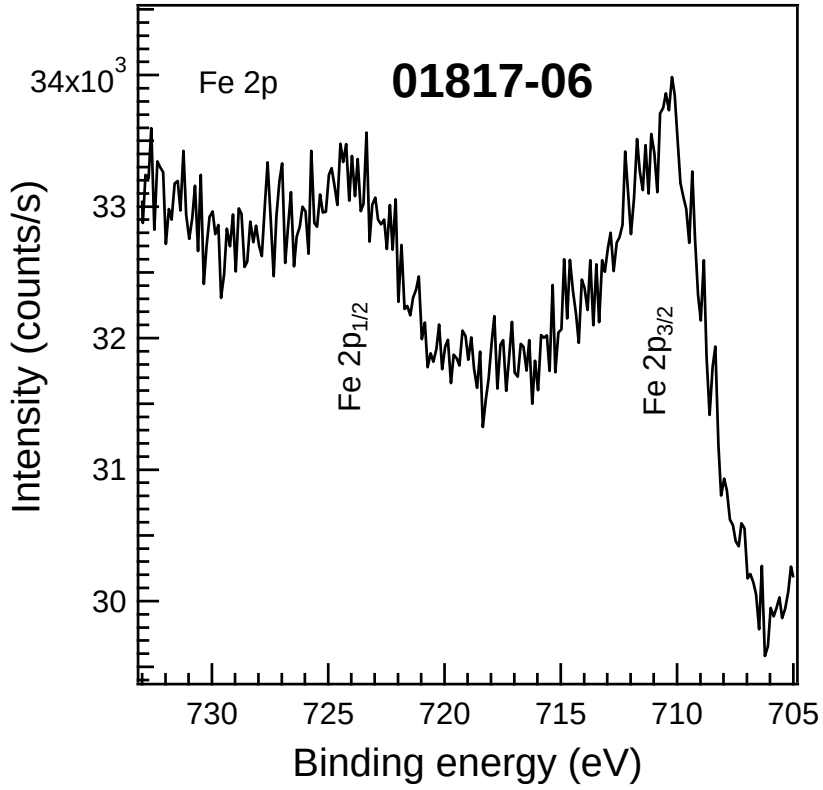

Publish in *SSS*: Yes ☒ No ☐

- **Accession #: 01817-06**
- **Host Material:** gCN-$CoFe_2O_4$
- **Technique:** XPS
- **Spectral Region:** Fe 2p

Instrument: Perkin-Elmer Physical Electronics, Inc. 5600ci
Excitation Source: Mg Ka
Source Energy: 1253.6 eV
Source Strength: 200 W
Source Size: >25 mm x >25 mm
Analyzer Type: spherical sector
Incident Angle: 9 °
Emission Angle: 45 °
Analyzer Pass Energy 58.7 eV
Analyzer Resolution: 0.6 eV
Total Signal Accumulation Time: 1284.0 s
Total Elapsed Time: 1412.4 s

Number of Scans: 80

Effective Detector Width: 0.6 eV